nature physics

LETTERS

PUBLISHED ONLINE: 25 NOVEMBER 2012 | DOI: 10.1038/NPHYS2492

Three-photon energy–time entanglement

L. K. Shalm[1]*, D. R. Hamel[1], Z. Yan[1], C. Simon[2], K. J. Resch[1] and T. Jennewein[1]*

Entangled quantum particles have correlations stronger than those allowed by classical physics. These correlations are at the heart of deep foundational questions in quantum mechanics[1–3], and form the basis of many emerging quantum technologies[4–9]. Although the discrete variables of up to 14 ions[10] and the continuous variables between three intense optical beams[11,12] have been entangled, it has remained an open challenge to entangle the continuous properties of three or more individual particles. Here we experimentally demonstrate genuine tripartite continuous-variable entanglement between three separated particles. In our set-up the three particles are photons created directly from a single input photon; the creation process leads to quantum correlations between the energies and emission times of the photons. The entanglement between our photons is the three-party generalization of the Einstein–Podolsky–Rosen[1] correlations for continuous variables, and could serve as a valuable resource in a wide variety of quantum information tasks.

We directly generate three entangled photons using the nonlinear process of cascaded spontaneous parametric downconversion (C-SPDC; ref. 13). In downconversion, a pump photon, with frequency ω_p, inside a nonlinear material will occasionally fission into a pair of daughter photons with frequencies ω_0 and ω_1. The total energy in the process is conserved[14] with $\hbar\omega_p = \hbar\omega_0 + \hbar\omega_1$. The daughter photons share strong energy and time correlations that are the hallmark of entanglement[15,16]. The SPDC process is repeated with one of these daughter photons, at ω_0, now serving as the pump, creating a pair of granddaughter photons simultaneously at ω_2 and ω_3. Again energy is conserved, and the total energy of the the three photons created in C-SPDC must sum to the energy of the pump: $\hbar\omega_p = \hbar\omega_1 + \hbar\omega_2 + \hbar\omega_3$. The simplified representation of our three-photon state in frequency space, assuming a monochromatic pump, has the form

$$\Psi_{\mathrm{CSPDC}} \approx \int_{\omega_1}\int_{\omega_2} \mathrm{d}\omega_1 \mathrm{d}\omega_2 G_1(\omega_1, \omega_p - \omega_1) \times G_2(\omega_2, \omega_p - \omega_1 - \omega_2) a_1^\dagger(\omega_1) a_2^\dagger(\omega_2) a_3^\dagger(\omega_p - \omega_1 - \omega_2)|0\rangle \quad (1)$$

where $G_1(\omega_1, \omega_p - \omega_1)$ and $G_2(\omega_2, \omega_p - \omega_1 - \omega_2)$ are the joint-spectral functions resulting from the phase-matching conditions of the first and second SPDC crystals respectively[17]. The three photons, consequently, share strong spectral correlations and exhibit genuine tripartite energy–time entanglement.

To verify the tripartite entanglement of the photons generated in our C-SPDC process we use continuous-variable entanglement criteria, which we derive based on the work in ref. 18, for position and momentum. Consider three separable particles each described by the dimensionless observables x_k, p_k $(k = 1, 2, 3)$ fulfilling the commutation relations $[x_k, p_l] = i\delta_{kl}$, where δ_{kl} is the Kronecker delta (note: in ref. 18 a different commutation relation is used).

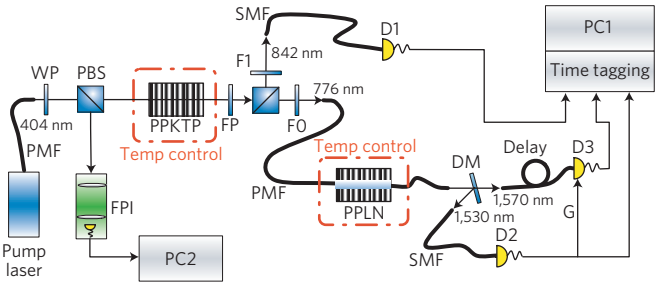

Figure 1 | Our three entangled photons are created using C-SPDC. A narrowband pump laser at 404 nm downconverts into a pair of orthogonally polarized photons at 842 and 776 nm inside a periodically-poled KTP crystal (PPKTP). A filter (FP) removes the remaining pump light. A polarizing beamsplitter (PBS) is used to separate the two photons, and narrowband filters, F0 and F1, are used to block stray light. The photon at 842 nm is coupled into a single-mode fibre (SMF) and sent to the single-photon detector D1. The photon at 776 nm is coupled into single-mode polarization maintaining fibre (PMF) and sent to a PPLN waveguide, where it downconverts into a pair of photons at 1530 and 1570 nm. The photons are outcoupled into free space, where a dichroic mirror (DM) is used to split the photons. The photons are then coupled back into single-mode fibre and sent to single-photon detectors D2 and D3 (see Methods for more information about the detectors). The signals from all three detectors are sent to a time-tagging unit, and a computer (PC1) is used to process coincidence events. A wave plate (WP) and PBS send part of the 404 nm pump to a Fabry-Perot Interferometer (FPI), controlled by a second computer (PC2), to continuously monitor its spectrum throughout the run.

Each individual particle must satisfy the uncertainty relationship $\Delta x_i \Delta p_i \geq 1/2$. Together, all three particles must satisfy the following position–momentum uncertainty inequalities (see Supplementary Information for details):

$$\Delta(x_2 - x_1)\Delta(p_1 + p_2 + p_3) \geq 1 \quad (2)$$

$$\Delta(x_3 - x_2)\Delta(p_1 + p_2 + p_3) \geq 1 \quad (3)$$

$$\Delta(x_3 - x_1)\Delta(p_1 + p_2 + p_3) \geq 1 \quad (4)$$

Violating any one of these inequalities is sufficient to demonstrate that a state contains some entanglement. Violating any two inequalities demonstrates that the state is fully inseparable[19]. For pure states, full inseparability implies genuine tripartite entanglement[20]. However, full inseparability and genuine tripartite entanglement are not, in general, the same thing. Mixtures of bipartite entangled states that are fully inseparable but not genuinely tripartite entangled are also capable of violating two

[1]Institute for Quantum Computing and Department of Physics and Astronomy, University of Waterloo, Waterloo, N2L 3G1, Canada, [2]Institute for Quantum Information Science and Department of Physics and Astronomy, University of Calgary, Calgary, Alberta, T2N 1N4, Canada. *e-mail: kshalm@uwaterloo.ca; tjennewe@uwaterloo.ca.

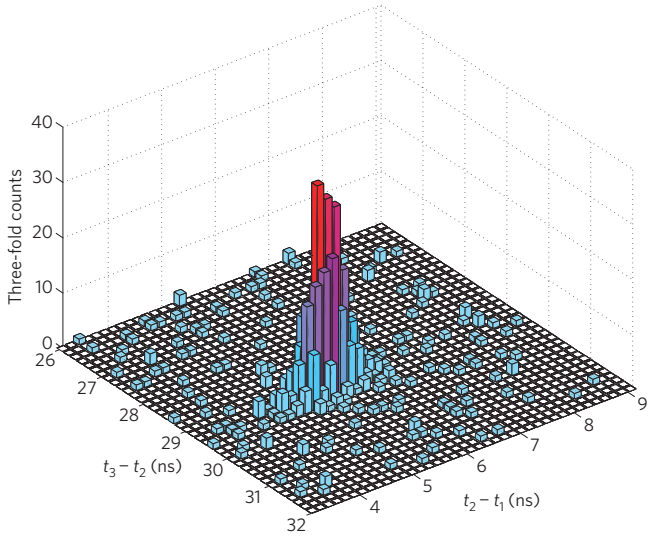

Figure 2 | 2D histogram of the difference in arrival times for the measured triple coincidences over 72.6 hours. The triple events are all localized to a small region of the histogram, indicating strong correlations in the arrival times of the three photons.

of the above inequalities. A more general entanglement criterion is therefore required to detect genuine tripartite entanglement. In the Supplementary Information we provide an overview of the definitions of full inseparability and genuine tripartite entanglement and derive the following inequalities:

$$[\Delta(x_2-x_1)+\Delta(x_3-x_1)]\,\Delta(p_1+p_2+p_3)\geq 1 \quad (5)$$

$$[\Delta(x_2-x_1)+\Delta(x_3-x_2)]\,\Delta(p_1+p_2+p_3)\geq 1 \quad (6)$$

$$[\Delta(x_3-x_2)+\Delta(x_3-x_1)]\,\Delta(p_1+p_2+p_3)\geq 1 \quad (7)$$

$$[\Delta(x_2-x_1)+\Delta(x_3-x_1)+\Delta(x_3-x_2)]\,\Delta(p_1+p_2+p_3)\geq 2 \quad (8)$$

Violating any one of them is sufficient to demonstrate genuine tripartite entanglement.

The position and momentum operators x and p are well-defined for narrow-band photons[21], such as those generated by our C-SPDC process, with the usual commutation relation $[x,p]=i$. Because photons propagate at the speed of light, c, measuring the arrival time, t, of a photon at a single-photon detector is equivalent to measuring its longitudinal position x ($t=x/c$), and measuring its frequency, ω, is equivalent to measuring its longitudinal momentum p ($\hbar\omega=cp$). Using this correspondence it is possible to write down the energy–time equivalents to the inequalities in equations (5)–(8):

$$[\Delta(t_2-t_1)+\Delta(t_3-t_1)]\,\Delta(\omega_1+\omega_2+\omega_3)\geq 1 \quad (9)$$

$$[\Delta(t_2-t_1)+\Delta(t_3-t_2)]\,\Delta(\omega_1+\omega_2+\omega_3)\geq 1 \quad (10)$$

$$[\Delta(t_3-t_2)+\Delta(t_3-t_1)]\,\Delta(\omega_1+\omega_2+\omega_3)\geq 1 \quad (11)$$

$$[\Delta(t_2-t_1)+\Delta(t_3-t_1)+\Delta(t_3-t_2)]\,\Delta(\omega_1+\omega_2+\omega_3)\geq 2 \quad (12)$$

States of the form in equation (1) can violate all the inequalities maximally, namely the left-hand side goes to zero, and thus exhibit genuine tripartite entanglement.

Measuring the difference in arrival times of the three photons using fast single-photon detectors gives the required timing uncertainties for testing the inequalities. However, directly measuring the frequencies of each individual photon with the precision needed (sub-gigahertz resolution over a bandwidth of several terahertz) to violate the inequalities is infeasible with current count rates. Instead we rely on the fact that energy is conserved in the process of downconversion. The energy of the pump is equal to the energy of the three daughter photons created in C-SPDC ($\hbar\omega_p=\hbar\omega_1+\hbar\omega_2+\hbar\omega_3$); measuring the frequency of the pump provides a direct mea-

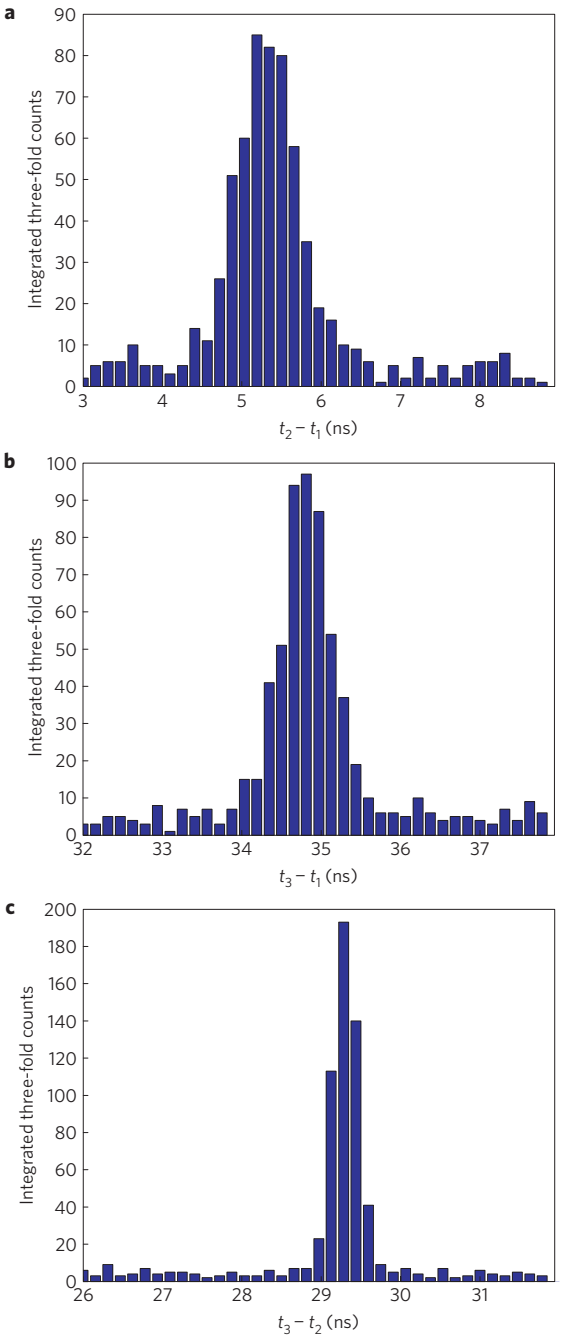

Figure 3 | Histograms of the difference in arrival times between two of the three photons measured over 72.6 hours. Each histogram is obtained by integrating the triples counts over the arrival time of the third photon to remove its dependence on the results. From this we find the uncertainty in the arrival times of the photons to be $\Delta(t_2-t_1)=0.37\pm0.02$ ns (**a**), $\Delta(t_3-t_2)=0.162\pm0.004$ ns (**b**) and $\Delta(t_3-t_1)=0.31\pm0.02$ ns (**c**). The timing uncertainties were verified using two-fold coincidence data that was obtained at the same time as the three-fold coincidence data (see Supplementary Information).

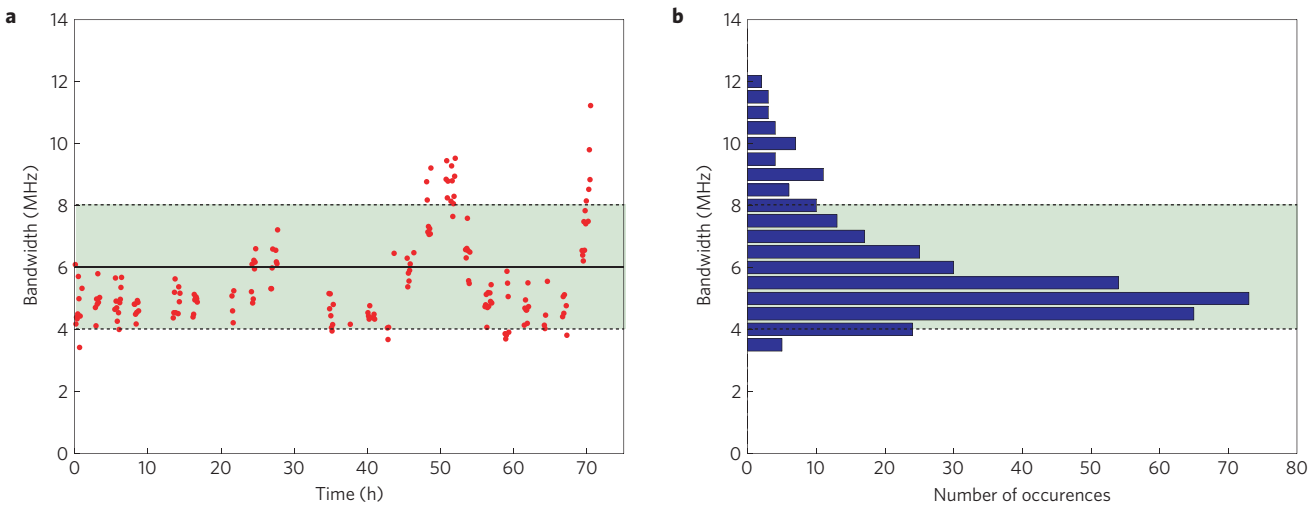

Figure 4 | Bandwidth of the pump photons as measured by a Fabry–Perot interferometer at five-minute intervals during the 72.6 hour run. a, The measured bandwidth as a function of time. The fluctuations in the measured bandwidths are the result of thermal drifts in the apparatus over the course of the run. **b**, Histogram of the measured pump bandwidths over the duration of the run. The average bandwidth is measured to be $\Delta\omega_p/2\pi = 6$ MHz with a standard deviation of 2 MHz (illustrated by the shaded regions in the graphs).

surement of the total frequency of the three daughter photons required by the inequalities. We experimentally verify that energy is conserved in downconverion in our high-efficiency periodically-poled lithium niobate (PPLN) waveguide, the central component of our experiment, using an unbalanced interferometer (see Supplementary Information for more details). Furthermore, energy (frequency) conservation in second-order nonlinear processes, such as downconversion, has been extensively verified using techniques such as Franson interferometry[15,16], and been measured down to a line width of 200 kHz, an uncertainty much smaller than the scale considered in our experiment, in second-harmonic generation[22,23] (the time-reversed process of SPDC).

To create our three entangled photons using C-SPDC (see Fig. 1), first a narrowband pump laser at 404 nm is used to produce a pair of non-degenerate SPDC photons at 776 and 842 nm. The photon at 776 nm is then sent through a second SPDC crystal, where a pair of granddaughter photons at 1530 and 1570 nm are generated (see Methods for more details). This process leaves the 842, 1530 and 1570 nm photons entangled in energy and time. Our set-up detects an average of 7 triples h^{-1}, from which we can infer the generation of 45 triples min^{-1} accounting for losses due to coupling and detection. To obtain sufficient photon counts with small statistical fluctuations, data was collected for a total of 72.6 hours.

The timing information from the detections was analysed, and the triple coincidence counts binned into a two-dimensional (2D) histogram based on $t_2 - t_1$ and $t_3 - t_2$, as shown in Fig. 2. From the histogram it is clear that the photon arrivals are tightly correlated in time. The uncertainty in the arrival time between any pair of photons can be found by integrating over the arrival time of the other photon, removing its dependence, as shown in Fig. 3. From these integrated histograms we find that $\Delta(t_2 - t_1) = 0.37 \pm 0.02$ ns, $\Delta(t_3 - t_2) = 0.162 \pm 0.004$ ns, and $\Delta(t_3 - t_1) = 0.31 \pm 0.02$ ns. Our measurements are limited by the timing jitter in our detectors and the resolution of our time-tagging unit (156 ps). The effect of the jitter can be clearly seen in the elliptical shape of the 2D arrival time histogram—the jitter on the detector used to detect the 842 nm photon is a factor of two larger than the jitter of the two telecom detectors. This is reflected in the uncertainty $\Delta(t_3 - t_2)$, which is approximately a factor of two smaller than either $\Delta(t_2 - t_1)$ or $\Delta(t_3 - t_1)$. Alternatively, we can study the two-photon coincidences between detectors D1 and D2, and D2 and D3, independent of the third detector (see Supplementary Information) to verify that integrating over the third photon yields the correct two-photon timing histograms. The need for gating with the 1570 nm detector (t_3) prevents the coincidences between t_3 and t_1 from being analysed independently of t_2, but the 50 ns gate width is much larger than the uncertainty in the arrival time of a photon, and approximates the response of a free-running detector.

It is possible for the first downconversion crystal to create two pairs of photons. To prevent two pump photons at 776 nm from reaching detectors D2 and D3 and creating a false triple, a spectral filter is used that blocks the pump light. Furthermore, the telecom detectors have a negligible efficiency at the pump wavelength. By tuning the temperature of the PPLN waveguide away from phasematching, we verified that the primary source of accidental triples is due to coincidences with detector dark counts[13].

Owing to energy conservation, the energy uncertainty of the photon triplets is given by the energy uncertainty in the 404 nm pump photons. To measure the uncertainty in the pump energy, a scanning Fabry–Perot interferometer (FPI) was used to continuously monitor the bandwidth of the 404 nm laser throughout the experiment. Owing to instabilities caused by temperature fluctuations, the measured bandwidth fluctuates over time, as shown in Fig. 4a, leading to the distribution in Fig. 4b. The average value and standard deviation of this distribution yield a pump bandwidth of $\Delta\omega_p/2\pi = (6 \pm 2)$ MHz.

The four measured time–bandwidth products for our three photons are

$$[\Delta(t_2 - t_1) + \Delta(t_3 - t_1)]\,\Delta(\omega_1 + \omega_2 + \omega_3) = 0.03 \pm 0.01 \quad (13)$$

$$[\Delta(t_2 - t_1) + \Delta(t_3 - t_2)]\,\Delta(\omega_1 + \omega_2 + \omega_3) = 0.02 \pm 0.01 \quad (14)$$

$$[\Delta(t_3 - t_2) + \Delta(t_3 - t_1)]\,\Delta(\omega_1 + \omega_2 + \omega_3) = 0.018 \pm 0.005 \quad (15)$$

$$[\Delta(t_2 - t_1) + \Delta(t_3 - t_1) + \Delta(t_3 - t_2)]\,\Delta(\omega_1 + \omega_2 + \omega_3) = 0.03 \pm 0.01 \quad (16)$$

Our three photons strongly violate inequalities (9)–(12) and are genuinely tripartite entangled. The state exhibits energy–time correlations close to the ideal state described in equation (1) where the time–bandwidth products are exactly zero. This state is the continuous-variable analogue to the famous Greenberger, Horne and Zeilinger entangled state[18,24], and the natural extension of the two-party continuous-variable Einstein–Podolsky–Rosen

state[15,16,25]. The limiting factor in our measurements is the several hundred picosecond timing jitter of our detectors. On the basis of the bandwidth of our downconverted photons, the arrival times of the three photons should have a fundamental uncertainty on the order of a picosecond. With the development of faster detectors we should be able to lower our measured values of the inequalities, which are already close to ideal, by over two orders of magnitude.

Recent improvements in telecom wavelength detectors[26] and advances in nonlinear materials promise to greatly increase our detected triples rate[27,28]. Furthermore, new techniques to enhance the strength of nonlinear effects[29,30] mean that our scheme can in principle be scaled up to larger photon numbers. A major advantage of our states is that the continuous-variable entanglement is distributed amongst three individual photons, each at a different, tunable, wavelengths, enabling the creation of hyper-entangled states that simultaneously take advantage of both discrete- and continuous-variable quantum correlations. This multiplexing of entanglement over multiple discrete and continuous degrees of freedom may have important applications in quantum communication tasks. For example, a slight modification to our set-up would enable a photon at 776 nm to be interfaced with an atomic storage medium such as rubidium while the remaining two photons are transmitted over telecom fibres to remote quantum nodes. This would open up new possibilities in the storage and distribution of quantum information needed for quantum computing, cryptography, and secret sharing, and could lead to new fundamental tests of quantum mechanics.

Methods

In our set-up (shown if Fig. 1) we use a grating-stabilized pump laser with a wavelength of 404 nm and a bandwidth of 5 MHz (Toptica Bluemode) to pump a 30 mm potassium titanyl phosphate (PPKTP) crystal phase matched for Type-II SPDC. A pair of orthogonally polarized signal and idler photons, at 842 nm and 776 nm respectively, are generated co-linearly, and a polarizing beam splitter (PBS) is used to separate them. The signal photon at 842 nm is coupled into an optical fibre and sent to a Si single-photon detector. With 12 mW of pump power, 10^6 signal photons s^{-1} are detected. The idler photon is fibre-coupled and sent to a second SPDC crystal, a 30 mm Type-I phase matched PPLN waveguide (HC Photonics), where it splits into a pair of granddaughter photons at 1570 and 1530 nm. These granddaughter photons are outcoupled into free space and then split using a dichroic mirror. The photon at 1530 nm is sent to a self-built free-running InGaAs/InP-Avalanche Photo Diodes[31] (Princeton Lightwave, Negative Feedback Avalanche Diode - NFAD) detector cooled to 193 K, operating at 10% efficiency with approximately 100 dark counts s^{-1}. This detector is used to gate a second InGaAs/InP detector (iD Quantique, id201-SMF-ULN) operating at 25% detection efficiency with a 50 ns gate window to detect the granddaughter photon at 1570 nm. The gated detector had a much higher dark count rate of approximately 5×10^{-5} dark counts/(ns of gate). The arrival times of each photon in the three detectors are recorded by a time-tagging system (DotFast/UQDevices) with 156 ps resolution. In this way all the timing statistics from the two-fold and three-fold coincidence events generated by the C-SPDC process can be measured.

Received 8 March 2012; accepted 24 October 2012; published online 25 November 2012

References

1. Einstein, A., Podolsky, B. & Rosen, N. Can quantum-mechanical description of physical reality be considered complete? *Phys. Rev.* **47,** 777–780 (1935).
2. Bell, J. S. On the Einstein Podolsky Rosen paradox. *Physics* **1,** 195–200 (1964).
3. Aspect, A., Grangier, P. & Roger, G. Experimental realization of Einstein-Podolsky-Rosen-Bohm gedankenexperiment: A new violation of Bell's inequalities. *Phys. Rev. Lett.* **49,** 91–94 (1982).
4. Nielsen, M. A. & Chuang, I. L. *Quantum Computation and Quantum Information* (Cambridge Univ. Press, 2000).
5. Ekert, A. K. Quantum cryptography based on Bell's theorem. *Phys. Rev. Lett.* **67,** 661–663 (1991).
6. Briegel, H-J., Dür, W., Cirac, J. I. & Zoller, P. Quantum repeaters: The role of imperfect local operations in quantum communication. *Phys. Rev. Lett.* **81,** 5932–5935 (1998).
7. Goda, K. *et al.* A quantum-enhanced prototype gravitational-wave detector. *Nature Phys.* **4,** 472–476 (2008).
8. Hage, B. *et al.* Preparation of distilled and purified continuous-variable entangled states. *Nature Phys.* **4,** 915–918 (2008).
9. Ye, J., Kimble, H. & Katori, H. Quantum state engineering and precision metrology using state-insensitive light traps. *Science* **320,** 1734–1738 (2008).
10. Monz, T. *et al.* 14-qubit entanglement: Creation and coherence. *Phys. Rev. Lett.* **106,** 130506 (2011).
11. Aoki, T. *et al.* Experimental creation of a fully inseparable tripartite continuous-variable state. *Phys. Rev. Lett.* **91,** 080404 (2003).
12. Coelho, A. S. *et al.* Three-color entanglement. *Science* **326,** 823–826 (2009).
13. Hübel, H. *et al.* Direct generation of photon triplets using cascaded photon-pair sources. *Nature* **466,** 601–603 (2010).
14. Keller, T. E. & Rubin, M. H. Theory of two-photon entanglement for spontaneous parametric down-conversion driven by a narrow pump pulse. *Phys. Rev. A* **56,** 1534–1541 (1997).
15. Franson, J. Bell inequality for position and time. *Phys. Rev. Lett.* **62,** 2205–2208 (1989).
16. Kwiat, P. G., Steinberg, A. M. & Chiao, R. Y. High-visibility interference in a Bell-inequality experiment for energy and time. *Phys. Rev. A* **47,** 2472–2475 (1993).
17. Keller, T. E., Rubin, M. H., Shih, Y. & Wu, L-A. Theory of the three-photon entangled state. *Phys. Rev. A* **57,** 2076–2079 (1998).
18. van Loock, P. & Furusawa, A. Detecting genuine multipartite continuous-variable entanglement. *Phys. Rev. A* **67,** 052315 (2003).
19. Dür, W., Cirac, J. I. & Tarrach, R. Separability and distillability of multiparticle quantum systems. *Phys. Rev. Lett.* **83,** 3562–3565 (1999).
20. Bourennane, M. *et al.* Experimental detection of multipartite entanglement using witness operators. *Phys. Rev. Lett.* **92,** 087902 (2004).
21. Fedorov, M. *et al.* Spontaneous emission of a photon: Wave-packet structures and atom-photon entanglement. *Phys. Rev. A* **72,** 032110 (2005).
22. Sun, J., Gale, B. J. S. & Reid, D. T. Testing the energy conservation law in an optical parametric oscillator using phase-controlled femtosecond pulses. *Opt. Express* **15,** 4378–4384 (2007).
23. Ikegami, T., Slyusarev, S., Ohshima, S. & Sakuma, E. Accuracy of an optical parametric oscillator as an optical frequency divider. *Opt. Commun.* **127,** 69–72 (1996).
24. Greenberger, D. M., Horne, M. A. & Zeilinger, A. in *Bell's Theorem, Quantum Theory, and Conceptions of the Universe* (ed. Kafatos, M.) 73–76 (Kluwer, 1989).
25. Howell, J. C., Bennink, R. S., Bentley, S. J. & Boyd, R. W. Realization of the Einstein-Podolsky-Rosen paradox using momentum- and position-entangled photons from spontaneous parametric down conversion. *Phys. Rev. Lett.* **92,** 210403 (2004).
26. Collins, R. J., Hadfield, R. H. & Buller, G. S. Commentary: New developments in single photon detection in the short wavelength infrared regime. *J. Nanophoton.* **4,** 040301 (2010).
27. Corona, M., Garay-Palmett, K. & U'Ren, A. B. Experimental proposal for the generation of entangled photon triplets by third-order spontaneous parametric downconversion in optical fibers. *Opt. Lett.* **36,** 190–192 (2011).
28. Richard, S., Bencheikh, K., Boulanger, B. & Levenson, J. A. Semiclassical model of triple photons generation in optical fibers. *Opt. Lett.* **36,** 3000–3002 (2011).
29. Sangouard, N. *et al.* Faithful entanglement swapping based on sum-frequency generation. *Phys. Rev. Lett.* **106,** 120403 (2011).
30. Langford, N. K. *et al.* Efficient quantum computing using coherent photon conversion. *Nature* **478,** 360–363 (2011).
31. Yan, Z. *et al.* An ultra-low noise telecom wavelength free running single photon detector using negative feedback avalanche diode. *Rev. Sci. Instrum.* **83,** 073105 (2012).

Acknowledgements

We thank the Ontario Ministry of Research and Innovation ERA, QuantumWorks, NSERC, OCE, Industry Canada, Canadian Institute for Advanced Research (CIFAR) and CFI for financial support. C.S. acknowledges support by an Alberta Innovates Technology Futures (AITF) New Faculty Award. We thank B. Boulanger and A. M. Steinberg for useful discussions.

Author contributions

L.K.S. and D.R.H. carried out the experiment. C.S., K.J.R. and T.J. conceived the experiment. Z.Y. developed the detectors and electronics used in the experiment. Data was analysed by L.K.S., D.R.H., K.J.R., and T.J. All authors contributed to the writing of the manuscript.

Additional information

Supplementary information is available in the online version of the paper. Reprints and permissions information is available online at www.nature.com/reprints. Correspondence and requests for materials should be addressed to L.K.S. or T.J.

Competing financial interests

The authors declare no competing financial interests.